

Solubility Differences of Halocarbon Isomers in Ionic Liquid [emim][Tf₂N]

Mark B. Shiflett*[†] and A. Yokozeki[‡]

DuPont Central Research and Development, Experimental Station E304, Wilmington, Delaware 19880, and DuPont Fluoroproducts Laboratory, Chestnut Run Plaza 711, Wilmington, Delaware 19880

Solubility behaviors of CFC-113 (CFCl₂–CF₂Cl), CFC-113a (CCl₃–CF₃), CFC-114 (CF₂Cl–CF₂Cl), CFC-114a (CFCl₂–CF₃), HCFC-123 (CHCl₂–CF₃), HCFC-123a (CHClF–CF₂Cl), HCFC-124 (CHFCl–CF₃), HCFC-124a (CHF₂–CF₂Cl), HFC-134 (CHF₂–CHF₂), and HFC-134a (CH₂F–CF₃) in room-temperature ionic liquid 1-ethyl-3-methylimidazolium bis(trifluoromethylsulfonyl)imide ([emim][Tf₂N]) have been investigated using a gravimetric microbalance method from (283 to 348) K or volumetric and cloud-point methods. In the case of the perhalogenated compounds (CFC-113, CFC-114, and their isomers), the solubility behavior between isomers in the ionic liquid is practically identical with large immiscibility gaps. This suggests that the (present) ionic liquid cannot be used for these isomer separations. However, the monohydrogen substituted halocarbons (HCFC-123, HCFC-124, and their isomers) begin to show some difference (liquid–liquid immiscibility gap) in the ionic liquid. The isomer effect on the solubility in the ionic liquid becomes significant for the dihydrogen-substituted halocarbons (HFC-134 and HFC-134a), and these isomers can be separated using [emim][Tf₂N] as an entrainer in an extractive distillation. This observation is consistent with our earlier findings for various HFCs in ionic liquids.

Introduction

Ionic liquids as a new type of solvent are being studied for a variety of separation applications.^{1–12} In particular, isomer separations⁴ are often required in the chemical and pharmaceutical industries. Often isomers have similar thermophysical properties (e.g., normal boiling point), which make it difficult to separate using conventional techniques such as distillation. The present study was initiated to find out whether room-temperature ionic liquids (RTILs) could separate halocarbon isomers. In addition to the practical application, we are motivated to gain more fundamental understanding about the solubility behavior (or molecular interactions) of this class of compounds in RTILs. The present report is a continuation of our previous studies on the vapor–liquid equilibrium (VLE) and liquid–liquid equilibrium (LLE) of halocarbons in RTILs.^{13–21} In this work, we investigate three classes of halocarbons: chlorofluorocarbons (CFCs), hydrochlorofluorocarbons (HCFCs), and hydrofluorocarbons (HFCs) in RTILs. We have systematically studied five isomer pairs and have prepared binary mixtures of 1,1,2-trichloro-1,2,2-trifluoroethane (CFC-113, CFCl₂–CF₂Cl) and 1,1,1-trichloro-2,2,2-trifluoroethane (CFC-113a, CCl₃–CF₃); 1,2-dichloro-1,1,2,2-tetrafluoroethane (CFC-114, CF₂Cl–CF₂Cl) and 1,1-dichloro-1,2,2,2-tetrafluoroethane (CFC-114a, CFCl₂–CF₃); 1,1-dichloro-2,2,2-trifluoroethane (HCFC-123, CHCl₂–CF₃) and 1,2-dichloro-1,2,2-trifluoroethane (HCFC-123a, CHClF–CF₂Cl); 1-chloro-1,2,2,2-tetrafluoroethane (HCFC-124, CHFCl–CF₃) and 2-chloro-1,1,2,2-tetrafluoroethane (HCFC-124a, CHF₂–CF₂Cl); and 1,1,2,2-tetrafluoroethane (HFC-134, CHF₂–CHF₂) and 1,2,2,2-tetrafluoroethane (HFC-134a, CH₂F–CF₃) with room-temperature ionic liquid 1-ethyl-3-methylimidazolium bis(trifluoromethylsulfonyl)imide ([emim][Tf₂N]). The chemical structure for [emim][Tf₂N] is shown in Figure 1.

* Corresponding author. E-mail: mark.b.shiflett@usa.dupont.com.

[†] DuPont Central Research and Development.

[‡] DuPont Fluoroproducts Laboratory.

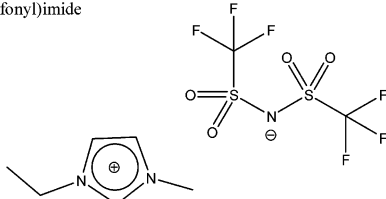
Chemical Name	Abbreviation	Structure	Molar Mass
1-ethyl-3-methylimidazolium bis(trifluoromethylsulfonyl)imide	[emim][Tf ₂ N]		391.31

Figure 1. Chemical structure of ionic liquid [emim][Tf₂N].

For the halocarbons with a sufficient vapor pressure (CFC-114, CFC-114a, HCFC-124, HCFC-124a, HFC-134, and HFC-134a), we use the gravimetric microbalance at a temperature range of (283 to 348) K for VLE measurements, whereas for low vapor pressure halocarbons (CFC-113, CFC-113a, HCFC-123, and HCFC-123a), we use only the volumetric or cloud-point method for LLE measurements. VLE data (CFC-114 isomers, HCFC-124 isomers, and HFC-134 isomers) have been well correlated with an EOS model.^{19,22} The EOS model has been used to predict the liquid–liquid-phase boundary which has been confirmed. Experimental LLE data (CFC-113 isomers and HCFC-123 isomers) have been well correlated by the NRTL (nonrandom two liquid) activity coefficient model.^{13,23,24}

Experimental

Materials. CFC-113 (CAS registry no. 76-13-1), CFC-113a (CAS registry no. 354-58-5), CFC-114 (CAS registry no. 76-14-2), CFC-114a (CAS registry no. 374-07-2), HCFC-123 (CAS registry no. 306-83-2), HCFC-124 (CAS registry no. 2837-89-0), HCFC-124a (CAS registry no. 354-25-6), and HFC-134a (CAS registry no. 811-97-2) were obtained from DuPont Fluoroproducts (Wilmington, DE). HCFC-123a (product and lot no. 1100-7-11 Q9B-64, CAS registry no. 354-23-4) was obtained from SynQuest Laboratory, Inc. (Alachua, FL), and HFC-134 (lot no. 0221TA06, CAS registry no. 359-35-3) was obtained

Table 1. Properties of Halocarbon Compounds and Sample Purity Analysis

compd	formula	T_b /K	T_c /K	purity ^g /%	impurities ^h /%
CFC-113	CFCl ₂ -CF ₂ Cl	320.74 ^{a,b}	487.21 ^b	> 99.99	trace isomers
CFC-113a	CCl ₃ -CF ₃	319.31 ^c	483.42 ^c	99.4	0.4 R-113, 0.1 R-114a, 0.1 other isomers
CFC-114	CF ₂ Cl-CF ₂ Cl	276.74 ^b	418.86 ^d	97.3	1.9 R-115, 0.4 R-12/R-22, 0.1 R-113, 0.1 R-123, 0.2 other isomers
CFC-114a	CFCl ₂ -CF ₃	276.59 ^a	418.60 ^d	99.1	0.6 R-123, 0.3 other isomers
HCFC-123	CHCl ₂ -CF ₃	300.97 ^b	456.83 ^b	97.6	1.0 R-123a, 1.0 R-4310, 0.4 other isomers
HCFC-123a	CHClF-CF ₂ Cl	301.35 ^f	461.6 ^e	98.3	0.4 R-123, 0.3 R-114, 0.5 unsaturates, 0.5 other isomers
HCFC-124	CHFCl-CF ₃	261.19 ^{a,b}	395.43 ^b	99.1	0.5 R-134, 0.2 R-22, 0.2 other isomers
HCFC-124a	CHF ₂ -CF ₂ Cl	261.38 ^a	399.90 ^d	99.0	0.5 R-134a, 0.2 R-245, 0.3 other isomers
HFC-134	CHF ₂ -CHF ₂	253.10 ^a	391.74 ^a	99.0	0.9 R-124, 0.1 other isomers
HFC-134a	CH ₂ F-CF ₃	247.08 ^b	374.21 ^b	99.6	0.3 R-143a, 0.1 other isomers

^a Ref 23. ^b Ref 28. ^c Ref 29. ^d Ref 30. ^e Ref 31. ^f Ref 33. ^g Mole percent analysis by GCMS; see text for details. ^h R is the abbreviation for refrigerant: R-115, chloropentafluoroethane; R-12, dichlorodifluoromethane; R-22, chlorodifluoromethane; R-4310, decafluoropentane; R-245, pentafluoropropane; R-143a, 1,1,1-trifluoroethane.

from Speciality Gases of America (Toledo, Ohio). The purity of these fluorocarbons was determined using a gas chromatography mass spectrometry (GCMS) method (Agilent 6890N, Restek Rtx-200 column, 105 m × 0.25 mm), and the results are shown in Table 1. The ionic liquid [emim][Tf₂N] (EMIM, electrochemical grade, assay ≥ 99.5 %, C₈H₁₁F₆N₃O₄S₂, lot and catalog no. 259095 IL-201-20-E, CAS registry no. 174899-82-2) was purchased from Covalent Associates Inc. (Woburn, MA). Methyl alcohol (assay ≥ 99.9 %, product and batch no. 646377-1L 05441CE, CAS registry no. 67-56-1) was obtained from Sigma-Aldrich, Inc. (St. Louis, MO) and used as a reference fluid for volumetric calibration of the experimental LLE apparatus.

The [emim][Tf₂N] sample was analyzed to verify the stated purity. The initial as-received mass fraction of water was measured by Karl Fischer titration (Aqua-Star C3000, solutions AquaStar Coulomat C and A). The sample contained a mass fraction of about 413·10⁻⁶ H₂O which is greater than what is stated on the manufacturer's website for electrochemical grade material (< 50 ppm).²⁵ A 20 mL sample of water was used to extract fluorine, chlorine, and bromine from 0.2 g of [emim]-[Tf₂N] at ambient temperature for 24 h. The extractable ions were measured by ion chromatography (column: DIONEX AS17; eluent: (0.4 to 50) mM NaOH; flow: 1.0 mL·min⁻¹; sample loop: 100 μL). The fluorine, chlorine, and bromine ions were found to be below the detection limit (< 5 μg·mL⁻¹). A 0.1886 g sample of [emim][Tf₂N] was combusted in a Wickbold torch, and the combustion gases were collected in water (99.86 mL) and analyzed by ion chromatography for total chlorine content. Two separate samples were analyzed and found to contain a mass fraction of (440 and 480)·10⁻⁶ chlorine (average (460 ± 20)·10⁻⁶).

Elemental analysis was performed by Schwarzkopf Microanalytical Laboratory, Inc. (Woodside, NY)²⁶ for carbon, hydrogen, fluorine, nitrogen, and sulfur content. Combining the results from each of the techniques described and shown in Table 2, we conclude that the [emim][Tf₂N] sample purity was ≥ 99.4 % which compares closely with the stated purity (≥ 99.5 %) by the manufacturer.

The [emim][Tf₂N] was dried and degassed by first filling a borosilicate glass tube with about 10 g of the ionic liquid and pulling a coarse vacuum with a diaphragm pump (Pfeiffer, model MVP055-3, Nashua, NH) for about 3 h. Next, the [emim]-[Tf₂N] was completely evacuated using a turbopump (Pfeiffer, model TSH-071) to a pressure of about 4·10⁻⁷ kPa while simultaneously heating and stirring the ionic liquid at a temperature of about 348 K for 5 days. The final mass fraction of water was again measured by Karl Fischer titration, and the dried sample contained 188·10⁻⁶ H₂O.

Experimental Method. A detailed description of the vapor-liquid equilibria (VLE) and liquid-liquid equilibria (LLE)

Table 2. Chemical Analysis of [emim][Tf₂N] Ionic Liquid

	units	[emim][Tf ₂ N]	
		calcd/reported	measured
assay		≥ 99.5 ^a	≥ 99.4
elemental			
C	%	24.55	24.60
H	%	2.83	3.02
F	%	29.13	29.70
N	%	10.74	10.75
S	%	16.39	17.05
O	%	16.35	NR ^b
H ₂ O ^c	·10 ⁻⁶	<50	413 ± 40
halogens			
F, Br, Cl ^e	·10 ⁻⁶		BDL ^d
Cl ^f	·10 ⁻⁶		460 ± 20

^a Ref 25. ^b Not reported. ^c Karl Fischer titration (mass fraction). ^d Below detection limit (< 5 μg·mL⁻¹). ^e Ion chromatography (extractable or soluble F, Br, Cl; mass fraction). ^f Wickbold torch (total Cl; mass fraction).

experimental equipment and procedures is available in our previous reports.^{17,18,22} Therefore, only the basic experimental techniques and measurement uncertainties are given here.

The gas solubility (VLE) measurements were made using a gravimetric microbalance (Hiden Isochema Ltd., IGA 003, Warrington, United Kingdom).²² A molecular sieve trap was installed to remove trace amounts of water from the halocarbons. Initially, about (60 to 70) mg of [emim][Tf₂N] was loaded into the sample container and heated to 348.15 K under a vacuum of about 10⁻⁹ MPa for 10 h to remove any trace amounts of water or other volatile impurities. No measurable mass loss was detected during drying which is consistent with the initial low water mass fraction (188·10⁻⁶).

The IGA003 apparatus can operate in both dynamic (continuous gas flow) and static (intermittent gas flow) modes. In this study, absorption measurements were performed in the static mode. The sample temperature was measured with a platinum resistance thermometer (PRT) within an uncertainty of ± 0.1 K. The thermocouple was calibrated using a standard platinum resistance thermometer (SPRT model 5699, Hart Scientific, American Fork, UT, range (73 to 933) K) and readout (Blackstack model 1560 with SPRT module 2560). The Blackstack instrument and SPRT are a certified secondary temperature standard with a NIST traceable accuracy to ± 0.005 K. Pressures from (10⁻² to 0.35) MPa were measured using a piezo-resistive strain gauge (Druck, model PDCR4010) with an accuracy of ± 0.8 kPa. The Druck pressure transducer was calibrated against a Paroscientific model 760-6K (Redmond, WA) pressure transducer (range (0 to 41.5) MPa, serial no. 62724). This

Table 3. Experimental Solubility (*PTx*) Data for CFC-114 and CFC-114a + [emim][Tf₂N]

CFC-114 (1)/[emim][Tf ₂ N] (2)			CFC-114a (1)/[emim][Tf ₂ N] (2)		
<i>T</i> /K	<i>P</i> /MPa	100 <i>x</i> ₁	<i>T</i> /K	<i>P</i> /MPa	100 <i>x</i> ₁
283.1	0.0103	1.2	283.2	0.0102	1.3
283.0	0.0503	6.0	283.1	0.0503	6.6
283.1	0.0753	9.2	283.1	0.0754	10.1
283.1	0.1003	12.6	283.1	0.1003	14.2
298.0	0.0103	0.6	298.3	0.0104	0.6
298.2	0.0503	3.4	298.1	0.0504	3.2
298.3	0.0705	5.0	298.1	0.0705	4.8
298.1	0.1005	7.3	298.1	0.1005	7.3
298.2	0.1255	9.3	298.0	0.1254	9.5
298.1	0.1500	11.3	298.0	0.1503	11.7
323.0	0.0104	0.4	323.1	0.0104	0.2
323.1	0.0504	1.8	323.1	0.0504	1.7
323.1	0.0705	2.6	323.1	0.0705	2.5
323.1	0.1005	3.6	323.1	0.1003	3.7
323.1	0.1254	4.5	323.1	0.1254	4.7
323.1	0.1504	5.5	323.1	0.1502	5.7
348.1	0.0104	0.0	348.1	0.0105	0.1
348.1	0.0504	0.9	348.1	0.0504	1.0
348.1	0.0705	1.3	348.1	0.0705	1.5
348.1	0.1005	1.9	348.1	0.1005	2.1
348.1	0.1254	2.4	348.1	0.1254	2.7
348.1	0.1504	3.0	348.1	0.1504	3.2

instrument is a certified secondary pressure standard with a NIST traceable accuracy of 0.008 % of full scale.

Four isotherms were measured at about (283, 298, 323, and 348) K over a pressure range from about (0.01 to 0.15) MPa for CFC-114 and CFC-114a, (0.01 to 0.3) MPa for HCFC-124 and HCFC-124a, and (0.01 to 0.35) MPa for HFC-134 and HFC-134a. The upper pressure limit of the microbalance reactor was 2.0 MPa; however, the upper pressure limit for the halocarbon isomers was dependent on the saturation pressure (0.19 MPa, CFC-114 and CFC-114a; 0.34 MPa, HCFC-124; 0.31 MPa, HCFC-124a; 0.46 MPa, HFC-134; and 0.59 MPa, HFC-134a) in the sample container at ambient temperature (294.15 K). To ensure sufficient time for gas–liquid equilibrium, the ionic liquid samples were maintained at each pressure set point for a minimum of 3 h and a maximum of 10 h.

The instrumental uncertainties in *T* and *P* are within ± 0.1 K and ± 0.8 kPa, respectively. These uncertainties do not cause any significant effects in the gas solubility measurement. The total uncertainties in the solubility data due to both random and systematic errors have been estimated to be less than 0.006 mole fraction at given *T* and *P*. Another large source of uncertainty in the present solubility experiments is due to the buoyancy correction in the data analysis. Analysis of the buoyancy effects requires an accurate measurement of the [emim][Tf₂N] liquid density and halocarbon gas density. Liquid density data for [emim][Tf₂N] were measured by Kruppen et al.²⁷ and were used in our analysis. The liquid density data were correlated as d (g·cm⁻³) = 1.81638 - 9.97143·10⁻⁴ *T* (K) from (293 to 353) K. The NIST REFPROP²⁸ and our BLENDY EOS²⁹ programs were used to calculate the gas density. A detailed description of the buoyancy correction is provided in our previous report.²² The corrected solubility (*PTx*) data are shown in Tables 3 to 5.

LLE experiments have been made with these samples at constant temperatures from about (283 to 349) K using the volumetric method.^{17,18} Low-pressure sample containers were filled with dried [emim][Tf₂N] and halocarbons (CFC-113, CFC-113a, CFC-114, CFC-114a, HCFC-123, and HCFC-123a), and high-pressure sample containers were filled with dried [emim][Tf₂N] and halocarbons (HCFC-124, HCFC-124a, HFC-134, and HFC-134a) following the procedures outlined in our recent

Table 4. Experimental Solubility (*PTx*) Data for HCFC-124 and HCFC-124a + [emim][Tf₂N]

HCFC-124 (1)/[emim][Tf ₂ N] (2)			HCFC-124a (1)/[emim][Tf ₂ N] (2)		
<i>T</i> /K	<i>P</i> /MPa	100 <i>x</i> ₁	<i>T</i> /K	<i>P</i> /MPa	100 <i>x</i> ₁
283.0	0.0101	5.0	283.2	0.0103	4.7
283.2	0.0499	22.4	283.1	0.0503	21.2
283.1	0.0997	42.2	283.1	0.1001	40.1
283.1	0.1504	59.1	283.1	0.1503	57.3
283.1	0.1995	75.7	283.1	0.1999	75.9
298.1	0.0104	2.8	298.1	0.0104	2.9
298.2	0.0500	13.4	298.2	0.0503	12.8
298.0	0.1000	25.9	298.1	0.1004	24.4
298.2	0.1500	36.9	298.1	0.1501	35.6
298.1	0.2002	47.3	298.0	0.1993	46.1
298.2	0.2503	56.8	298.1	0.2503	57.2
298.1	0.3004	66.5	298.1	0.2996	69.2
323.1	0.0103	1.0	323.0	0.0104	1.2
323.1	0.0501	5.8	323.0	0.0502	5.8
323.1	0.1001	11.5	323.2	0.1003	11.6
323.1	0.1501	16.9	323.2	0.1502	17.1
323.1	0.1999	22.1	323.1	0.2003	22.2
323.1	0.2503	27.2	323.1	0.2504	27.1
323.1	0.3002	32.2	323.1	0.3001	32.2
348.1	0.0104	0.1	348.1	0.0105	0.1
348.1	0.0501	2.6	348.1	0.0502	2.7
348.1	0.1001	5.7	348.1	0.1004	5.7
348.1	0.1501	8.8	348.1	0.1503	8.7
348.1	0.1999	11.8	348.0	0.2002	11.6
348.1	0.2502	14.5	348.1	0.2496	14.3
348.1	0.3004	17.1	348.1	0.3001	17.1

Table 5. Experimental Solubility (*PTx*) Data for HFC-134 and HFC-134a + [emim][Tf₂N]

HFC-134 (1)/[emim][Tf ₂ N] (2)			HFC-134a (1)/[emim][Tf ₂ N] (2)		
<i>T</i> /K	<i>P</i> /MPa	100 <i>x</i> ₁	<i>T</i> /K	<i>P</i> /MPa	100 <i>x</i> ₁
282.9	0.0099	5.5	283.7	0.0100	1.9
283.2	0.0500	24.6	282.7	0.0499	10.5
283.1	0.1003	43.3	283.1	0.0998	21.9
283.2	0.1498	57.3	283.2	0.1498	31.8
283.0	0.1997	70.2	283.2	0.2003	41.5
283.1	0.2500	81.1	283.2	0.2501	51.6
283.2	0.3004	96.4	283.2	0.3005	61.3
—	—	—	283.2	0.3501	75.5
298.2	0.0099	3.3	298.2	0.0103	1.6
298.2	0.0500	15.6	298.1	0.0499	7.1
298.2	0.0999	28.4	298.1	0.1000	13.8
298.1	0.1496	39.5	298.1	0.1497	20.3
298.2	0.2001	49.0	298.1	0.2001	26.3
298.1	0.2496	57.3	298.2	0.2504	32.2
298.0	0.2995	64.8	298.1	0.3000	38.2
298.2	0.3497	71.6	298.1	0.3492	44.3
323.1	0.0102	1.6	323.1	0.0103	0.8
323.1	0.0500	7.6	323.1	0.0503	3.6
323.2	0.1004	14.7	323.1	0.1000	7.1
323.1	0.1505	21.0	323.1	0.1502	10.5
323.1	0.2004	26.9	323.1	0.2002	13.8
323.0	0.2494	32.3	323.0	0.2504	16.9
323.1	0.3003	37.4	323.2	0.3003	20.1
323.1	0.3505	42.1	323.1	0.3503	23.1
348.1	0.0105	0.6	348.1	0.0105	0.0
348.1	0.0504	4.0	348.1	0.0503	1.7
348.1	0.1005	7.9	348.1	0.1003	3.8
348.1	0.1505	11.6	348.1	0.1503	5.8
348.1	0.2004	15.2	348.1	0.2001	7.7
348.1	0.2500	18.6	348.1	0.2502	9.6
348.1	0.2996	21.9	348.1	0.3002	11.5
348.1	0.3505	25.0	348.1	0.3501	13.3

publications.^{17,18} Detail error analyses are also given in refs 17 and 18. The bath temperature was calibrated with the NIST traceable SPRT mentioned previously, and the uncertainty in temperature was ± 0.2 K. Special attention must be given to ensure no leaks occur from the sample containers after being filled with the high-pressure halocarbons. The mass of the sample containers were checked several times before starting

Table 6. LLE Data for the Halocarbon (CFC-113, CFC-113a, CFC-114, and CFC-114a) (1) + [emim][Tf₂N] (2) Systems^a

T			V'	V	V^E	V^E
K	$100x_1'$	$100x_1$	$\text{cm}^3\cdot\text{mol}^{-1}$	$\text{cm}^3\cdot\text{mol}^{-1}$	$\text{cm}^3\cdot\text{mol}^{-1}$	$\text{cm}^3\cdot\text{mol}^{-1}$
CFC-113 (1) + [emim][Tf ₂ N] (2)						
282.2 ± 0.2	100.0–0.2	22.0 ± 1.8	116.7 ± 0.6	222.4 ± 2.6	–0.4 ± 0.6	–2.3 ± 2.6
293.8 ± 0.2	100.0–0.2	23.0 ± 2.0	118.7 ± 0.6	223.0 ± 3.1	–0.6 ± 0.6	–2.3 ± 3.1
303.3 ± 0.2	100.0–0.2	23.0 ± 2.5	119.1 ± 0.5	223.1 ± 3.2	–1.5 ± 0.5	–5.3 ± 3.2
317.8 ± 0.2	100.0–0.2	23.3 ± 2.8	123.1 ± 0.7	220.0 ± 3.5	–1.5 ± 0.7	–6.0 ± 3.5
333.2 ± 0.2	23.7 ± 2.0	99.9 ± 0.1	221.8 ± 4.5	124.9 ± 0.7	–9.9 ± 4.5	–2.0 ± 0.7
343.2 ± 0.2	23.7 ± 2.0	100.0–0.2	223.7 ± 4.6	127.5 ± 0.5	–9.8 ± 4.6	–1.6 ± 0.5
CFC-113a (1) + [emim][Tf ₂ N] (2)						
293.8 ± 0.2	99.8 ± 0.2	24.3 ± 2.1	117.7 ± 0.8	220.1 ± 3.2	–1.2 ± 0.8	–3.4 ± 3.2
307.2 ± 0.2	99.6 ± 0.3	24.7 ± 2.0	121.2 ± 1.2	221.1 ± 2.7	–1.1 ± 1.2	–3.9 ± 2.7
317.8 ± 0.2	99.7 ± 0.3	24.6 ± 2.0	122.7 ± 1.4	223.2 ± 3.5	–1.3 ± 1.4	–4.3 ± 3.5
333.2 ± 0.2	24.9 ± 2.0	99.5 ± 0.5	223.5 ± 3.0	125.3 ± 1.4	–6.4 ± 3.0	–2.4 ± 1.4
343.2 ± 0.2	25.3 ± 2.0	99.6 ± 0.4	225.5 ± 3.0	127.5 ± 1.5	–6.0 ± 3.0	–2.5 ± 1.5
CFC-114 (1) + [emim][Tf ₂ N] (2)						
294.1 ± 0.2	18.7 ± 1.0	100.0–0.2	226.9 ± 2.0	115.3 ± 1.0	–3.9 ± 2.0	–0.3 ± 1.0
313.3 ± 0.2	19.0 ± 1.0	100.0–0.2	229.3 ± 2.7	120.9 ± 1.0	–4.8 ± 2.7	–0.4 ± 1.0
CFC-114a (1) + [emim][Tf ₂ N] (2)						
294.1 ± 0.2	17.9 ± 1.0	100.0–0.2	227.4 ± 2.4	116.0 ± 1.0	–4.6 ± 2.4	–0.4 ± 1.0
313.3 ± 0.2	18.6 ± 1.0	100.0–0.2	229.3 ± 1.5	120.8 ± 1.0	–5.3 ± 1.5	–0.5 ± 1.5

^a V' , observed molar volume, lower phase; V , observed molar volume, upper phase; V^E , excess molar volume, lower phase; V^E , excess molar volume, upper phase.

Table 7. LLE Data for Halocarbon (HCFC-123, HCFC-123a, HCFC-124, and HCFC-124a) (1) + [emim][Tf₂N] (2) Systems^a

T			V'	V	V^E	V^E
K	$100x_1'$	$100x_1$	$\text{cm}^3\cdot\text{mol}^{-1}$	$\text{cm}^3\cdot\text{mol}^{-1}$	$\text{cm}^3\cdot\text{mol}^{-1}$	$\text{cm}^3\cdot\text{mol}^{-1}$
HCFC-123 (1) + [emim][Tf ₂ N] (2)						
293.3 ± 0.2	83.6 ± 0.5	99.9 ± 0.1	125.2 ± 1.6	103.6 ± 0.5	–3.5 ± 1.6	–0.2 ± 0.5
313.2 ± 0.2	80.0 ± 0.5	99.9 ± 0.1	132.5 ± 2.2	107.4 ± 0.5	–5.5 ± 2.2	–0.3 ± 0.5
334.1 ± 0.2	76.3 ± 0.5	99.8 ± 0.2	141.7 ± 1.4	111.3 ± 0.8	–6.3 ± 1.4	–0.8 ± 0.8
HCFC-123a (1) + [emim][Tf ₂ N] (2)						
293.3 ± 0.2	88.2 ± 0.6	99.6 ± 0.4	118.0 ± 1.8	104.5 ± 1.1	–4.5 ± 1.8	–0.6 ± 1.1
313.2 ± 0.2	83.7 ± 0.7	99.6 ± 0.3	127.6 ± 1.8	107.3 ± 0.8	–5.2 ± 1.8	–1.2 ± 0.8
334.1 ± 0.2	79.2 ± 0.5	99.7 ± 0.3	137.4 ± 1.8	111.2 ± 1.0	–6.2 ± 1.8	–1.1 ± 1.0
HCFC-124 (1) + [emim][Tf ₂ N] (2)						
303.3 ± 0.2	84.1 ± 1.1	100.0–0.5	121.8 ± 3.2	102.0 ± 2.2	–5.1 ± 3.2	–0.1 ± 2.2
313.4 ± 0.2	82.0 ± 1.0	100.0–0.3	126.7 ± 3.0	105.0 ± 2.0	–6.2 ± 3.0	0.1 ± 2.0
330.2 ± 0.2	76.3 ± 1.0	100.0–0.2	136.9 ± 3.0	110.5 ± 1.6	–8.6 ± 3.0	–0.1 ± 1.6
HCFC-124a (1) + [emim][Tf ₂ N] (2)						
303.3 ± 0.2	83.8 ± 1.0	100.0–0.4	122.0 ± 3.6	101.9 ± 2.2	–5.3 ± 3.6	0.0 ± 2.2
313.4 ± 0.2	81.7 ± 0.8	100.0–0.3	128.1 ± 3.3	104.7 ± 1.8	–5.2 ± 3.3	–0.1 ± 1.8
330.2 ± 0.2	75.9 ± 1.0	100.0–0.2	141.0 ± 3.0	110.2 ± 1.5	–6.1 ± 3.0	–0.1 ± 1.5

^a V' , observed molar volume, lower phase; V , observed molar volume, upper phase; V^E , excess molar volume, lower phase; V^E , excess molar volume, upper phase.

Table 8. LLE Data for the Halocarbon (HFC-134a) (1) + [emim][Tf₂N] (2) System^a

T			V'	V	V^E	V^E
K	$100x_1'$	$100x_1$	$\text{cm}^3\cdot\text{mol}^{-1}$	$\text{cm}^3\cdot\text{mol}^{-1}$	$\text{cm}^3\cdot\text{mol}^{-1}$	$\text{cm}^3\cdot\text{mol}^{-1}$
HFC-134a (1) + [emim][Tf ₂ N] (2)						
333.5 ± 0.2	82.8 ± 0.3	99.0 ± 1.0	116.3 ± 1.6	98.5 ± 1.7	–9.4 ± 1.6	–0.2 ± 1.7
338.3 ± 0.2	81.0 ± 0.3	100.0–0.5	120.1 ± 1.6	99.6 ± 1.7	–10.8 ± 1.6	0.1 ± 1.7
345.2 ± 0.2	78.7 ± 0.3	100.0–0.5	124.9 ± 2.0	103.7 ± 1.9	–13.5 ± 2.0	0.0 ± 1.9
349.1 ± 0.2	77.3 ± 0.3	100.0–0.5	128.4 ± 2.2	106.4 ± 2.0	–14.5 ± 2.2	–0.1 ± 2.0

^a V' , observed molar volume, lower phase; V , observed molar volume, upper phase; V^E , excess molar volume, lower phase; V^E , excess molar volume, upper phase.

and after completing the LLE experiments to ensure that no halocarbons had escaped from the sample container. It is also important to mention that the vapor-phase density which contains halocarbons with a negligible contribution of [emim]-[Tf₂N] must be calculated using EOS programs^{28,29} and properly accounted for in the mass balance equations described in refs 17 and 18. Observed liquid-phase compositions and molar volumes are shown in Tables 6 to 8.

To prove the existence of a lower critical solution temperature (LCST) of the LLE curve, cloud-point measurements were made with binary mixtures prepared using the (HCFC-123, HCFC-124, and HFC-134) isomers + [emim][Tf₂N]. Four samples of both HCFC-123 isomers and [emim][Tf₂N] were prepared in low-pressure sample containers containing mole fractions from (80 to 95) % HCFC-123 isomers. Four samples of both HCFC-124 isomers and [emim][Tf₂N] were prepared in high-pressure

sample containers containing mole fractions from (80 to 95) % HCFC-124 isomers. Two samples of HFC-134a and one sample of HFC-134 and [emim][Tf₂N] were also prepared in high-pressure sample containers containing mole fractions from (85 to 95) % HFC-134 isomers. Starting at ambient temperature of about 293 K, for certain sample compositions where two liquid phases existed (some sample compositions were single phase at ambient temperature), the temperature was lowered (20 K·h⁻¹) with manual mixing in a constant temperature bath (Tamson Instruments, TV4000LT, Zoetermeer, Netherlands) until only a single phase existed for all the prepared mixtures. The bath temperature was calibrated with the NIST traceable SPRT mentioned previously, and the uncertainty in the bath temperature was ± 0.2 K. Once all the prepared samples were single phase, the temperature was slowly raised (5 K·h⁻¹) until a cloud layer became visible inside the glass sample tube. The temperature was recorded for each sample when the cloud layer formed. The liquid level in each tube at the cloud-point temperature must also be measured to calculate the vapor-phase volume. The vapor is assumed to contain only halocarbon, and using an EOS program^{28,29} the saturated vapor density was calculated at the cloud-point temperature to correct the amount of halocarbon in the liquid phase (reported cloud-point composition).

Results

Experimental Data. Experimental solubility (VLE and LLE) data are summarized in Tables 3 to 8. One of the most useful aspects of the present LLE method is the ability to obtain the molar volume of each separated liquid simultaneously with the mole fraction of each liquid at any given isothermal condition. Then, the excess molar volume (or volume of mixing) of each liquid solution (V^E and V^E) can be obtained, by use of the pure component molar volumes V_1^0 (halocarbon) and V_2^0 ([emim]-[Tf₂N]) using

$$V^E = V_m - x'_1 V_1^0 - x'_2 V_2^0 \text{ or } V^E = V_m - x_1 V_1^0 - x_2 V_2^0 \quad (1)$$

where V_m is the measured molar volume of the mixture ($V_m = V'$ for the lower phase L' or $V_m = V$ for the upper phase L), and (x'_1, x'_2 or x_1, x_2) are mole fractions of halocarbon (1) and [emim][Tf₂N] (2) in phase L' and L , respectively. Saturated liquid molar volumes for the halocarbons (CFC-113, CFC-113a, CFC-114, CFC-114a, HCFC-123, HCFC-124, HCFC-124a, HFC-134a) were calculated using EOS programs.^{28,29} Liquid molar volume for HCFC-123a was calculated from liquid density data.^{31–33} The molar volume for [emim][Tf₂N] was calculated from known liquid density data.²⁷

The vapor phase was initially assumed to contain only halocarbons (negligible vapor pressure for [emim][Tf₂N]). The uncertainty estimation for neglecting the moles of nitrogen in the vapor space during the LLE filling process (low-pressure sample containers) was calculated using the ideal gas law and an EOS program.²⁸ The vapor correction resulted in a small change in the liquid compositions ($\Delta x_1 = 0.1$ % and $\Delta x'_1 = 0.02$ %) and molar volumes ($\Delta V = 0.2$ cm³·mol⁻¹ and $\Delta V' = 0.1$ cm³·mol⁻¹); therefore, our assumption to neglect the nitrogen in the LLE sample container may be justified in this case. Total uncertainties in the final composition and molar volume determination are provided in Tables 6 to 8. Total uncertainties ($\delta x_{TE} = \sqrt{\delta x_{RE}^2 + \delta x_{SE}^2}$) were estimated by calculating both the overall random (δx_{RE}) and systematic errors (δx_{SE}). The following experimental parameters were considered to have an effect on the random errors: sample container calibration constants, mass of halocarbon and [emim][Tf₂N], and height

of lower and upper phases. The heights had the largest overall effect. The systematic errors include properly correcting for the area expansion, meniscus, and vapor-phase moles. For additional details on estimation of total errors, see refs 16 and 17.

Cloud-point measurements were visually determined for isomers of HCFC-123, HCFC-124, and HFC-134 with [emim]-[Tf₂N]. Cloud points were measured for HCFC-123 + [emim]-[Tf₂N] containing mole fractions of (80.0, 84.9, 89.8, and 95.0) % HCFC-123 at (313.3 ± 1) K, (289.2 ± 1) K, (264.2 ± 1) K, and (247.2 ± 2) K, respectively. Cloud points were measured for mixtures of HCFC-123a + [emim][Tf₂N] containing mole fractions of (80.0, 85.0, 89.8, and 95.0) % HCFC-123a at (330.2 ± 1) K, (308.0 ± 1) K, (291.2 ± 1) K, and (284.2 ± 1) K, respectively. It was particularly interesting to watch the second phase appear for the mixtures containing a mole fraction of 95 % HCFC-123 and HCFC-123a which are at about the lower critical solution composition. In these two cases, no cloud appeared, but rather the meniscus formed in the center of the single-phase liquid. Cloud points were measured for mixtures of HCFC-124 + [emim][Tf₂N] containing mole fractions of (79.3, 84.7, 89.9, and 94.5) % HCFC-124 at (318.2 ± 2) K, (302.2 ± 2) K, (286.2 ± 2) K, and (285.9 ± 1) K, respectively. Cloud points were measured for mixtures of HCFC-124a + [emim][Tf₂N] containing mole fractions of (79.4, 84.1, 89.8, and 95.5) % HCFC-124a at (318.2 ± 2) K, (307.2 ± 2) K, (278.2 ± 2) K, and (284.8 ± 1) K, respectively. Finally, a single cloud point was measured to prove the LCST behavior predicted by the EOS model for a mixture of HFC-134 + [emim][Tf₂N] containing a mole fraction of 91.2 % HFC-134. A cloud point was observed at (362.2 ± 1) K. Two mixtures of HFC-134a + [emim][Tf₂N] containing mole fractions of (84.0 and 94.7) % HFC-134a were prepared, and cloud points were observed at (329.2 ± 1) K and (330.2 ± 1) K, respectively.

Thermodynamic Model Analysis. In this study, we have employed a generic RK (Redlich–Kwong) type of cubic equation of state (EOS)^{19,22} to model the VLE for high-pressure halocarbons (CFC-114, HCFC-124, HFC-134, and their isomers) and predict the LLE. Observed LLE data for low-pressure halocarbons (CFC-113, HCFC-123, and their isomers) have been modeled with the NRTL (nonrandom two liquids) solution model.^{13,23,24} Details for both thermodynamic models are given in the Supporting Information. EOS model calculations with the present experimental data are shown in Figures 2 to 4 for HFC-134 isomers, HCFC-124 isomers, and CFC-114 isomers, respectively. NRTL model calculations and the measured experimental data are shown in Figures 5 and 6 for HCFC-123 isomers and CFC-113 isomers, respectively. Pure component EOS constants (Table S1), optimal binary interaction parameters (Table S2), and NRTL binary interaction parameters (Table S3) are given in the Supporting Information.

Discussion

All binary systems of the present study have shown partial immiscibilities, and particularly for the perhalogenated compounds (CFC-113, CFC-113a, and CFC-114, CFC-114a), the immiscibility gaps are very wide and nearly identical for the respective isomers. The minor differences observed for the other isomer pairs (HCFC-123 and HCFC-124) also make separation impractical for the halocarbon isomers using [emim][Tf₂N], although the possibility exists for other RTILs which may be useful for such separations. However, for the case of the HFC-134 isomers, the difference in solubility of the two isomers in the present RTIL is large enough that separation using [emim]-[Tf₂N] as an entrainer in an extractive distillation application will be quite practical.

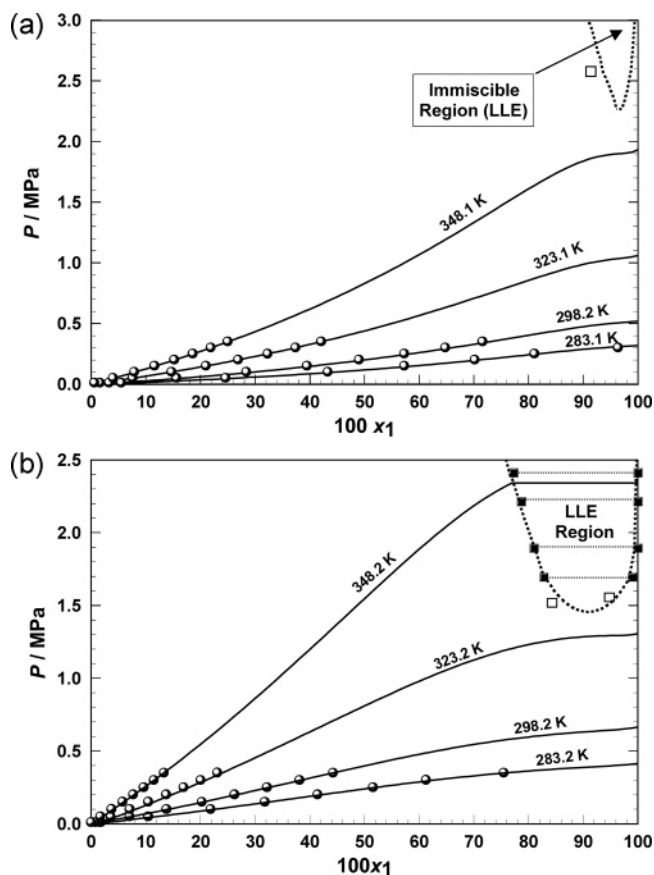


Figure 2. PT_x phase diagram of the (a) HFC-134 (1) + [emim][Tf_2N] (2) system and the (b) HFC-134a (1) + [emim][Tf_2N] (2) system: solid and dotted lines, calculated by the present EOS model; solid circles, the present experimental VLE data; solid squares and broken horizontal lines, the present experimental LLE data and the LLE tie lines; open squares, the observed cloud-point measurements.

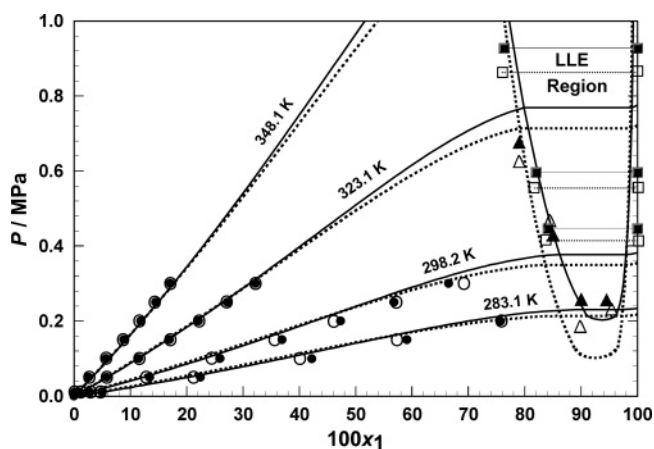


Figure 3. PT_x phase diagram of the HCFC-124 (HCFC-124a) (1) + [emim][Tf_2N] (2) system: solid (HCFC-124) and dotted (HCFC-124a) lines, calculated by the present EOS model; solid (HCFC-124) and open (HCFC-124a) circles, the present experimental VLE data; solid (HCFC-124) and open (HCFC-124a) squares and solid (HCFC-124) and broken (HCFC-124a) horizontal lines, the present experimental LLE data and the LLE tie lines; solid (HCFC-124) and open (HCFC-124a) triangles, the observed cloud-point measurements.

Figures 2 to 6 clearly show the dramatic effect in solubility by the hydrogen substitutions (Cl \rightarrow H): CFC-113 \rightarrow HCFC-123a, CFC-113a \rightarrow HCFC-123, CFC-114a \rightarrow HCFC-124, CFC-114 \rightarrow HCFC-124a, HCFC-124 \rightarrow HFC-134a, and HCFC-124a \rightarrow HFC-134. Similar hydrogen-substitution effects are known in other systems such as tetrafluoromethane (CF₄, PFC-14) \rightarrow

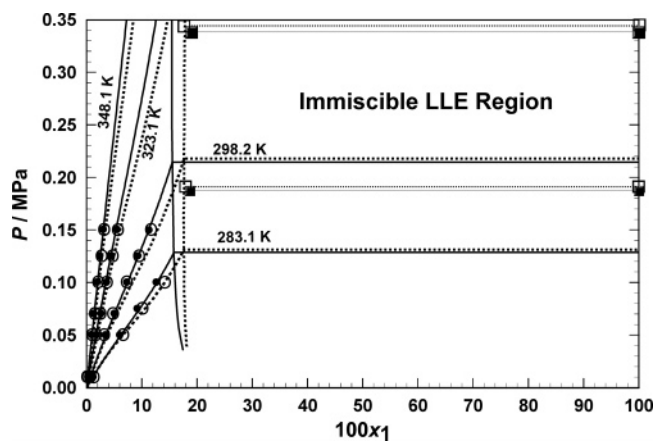


Figure 4. PT_x phase diagram of the CFC-114 (CFC-114a) (1) + [emim][Tf_2N] (2) system: solid (CFC-114) and dotted (CFC-114a) lines, calculated by the present EOS model; solid (CFC-114) and open (CFC-114a) circles, the present experimental VLE data; solid (CFC-114) and open (CFC-114a) squares and solid (CFC-114) and broken (CFC-114a) horizontal lines, the present experimental LLE data and the LLE tie lines.

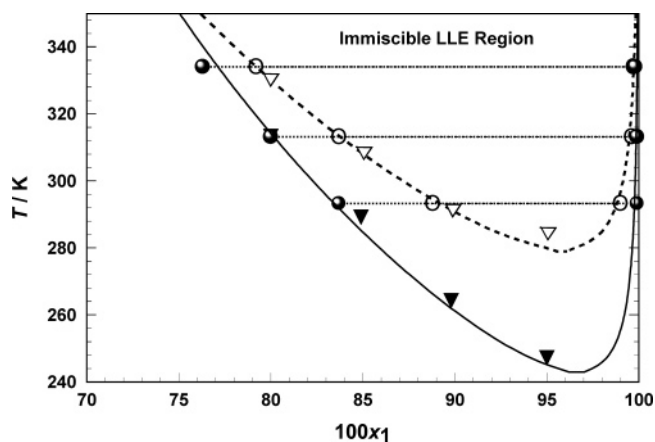


Figure 5. T_x phase diagram of the HCFC-123 (HCFC-123a) (1) + [emim][Tf_2N] (2) system: solid (HCFC-123) and open (HCFC-123a) circles, experimental LLE data; solid (HCFC-123) and dotted (HCFC-123a) lines, the present NRTL model calculations; broken (HCFC-123 and HCFC-123a overlap) horizontal lines, experimental LLE tie lines; solid (HCFC-123) and open (HCFC-123a) triangles, the observed cloud-point measurements.

trifluoromethane (CHF₃, HFC-23), dichlorodifluoromethane (CCl₂F₂, CFC-12) \rightarrow chlorodifluoromethane (CHClF₂, HCFC-22), and chloropentafluoroethane (CClF₂-CF₃, CFC-115) \rightarrow pentafluoroethane (CHF₂-CF₃, HFC-125).^{21,24}

At first glance, these solubility differences are surprising, by considering the fact that the same type of compounds usually show similar VLE and LLE behaviors in a given type of solvent. It is interesting to note that the solubility difference does correlate with the magnitude of the dipole moments of CFC-114 (0.658 D), CFC-113 (0.803 D), HCFC-123 (1.356 D), HCFC-124 (1.469 D), and HFC-134a (2.058 D).²⁸ However, we have found in our previous work that this is not always the case (e.g., CH₂F₂, HFC-32, 1.978 D is more soluble than CH₃-CF₃, HFC-143a, 2.340 D in [bmim][PF₆]).¹³ Another important property of hydrogen-containing fluorocarbons is the ability to form hydrogen bonds (H-F-H) with an ionic liquid, and this affects the solubility behavior.¹³⁻²¹

For the cases of (HCFC-123, HCFC-124, and HFC-134) isomers, the existence of a LCST was examined by the well-known cloud-point method over a wide temperature range [(247 to 362) K]. For the cases of HCFC-123 and HCFC-123a + [emim][Tf_2N], we have calculated LCSTs at about (243 \pm 1)

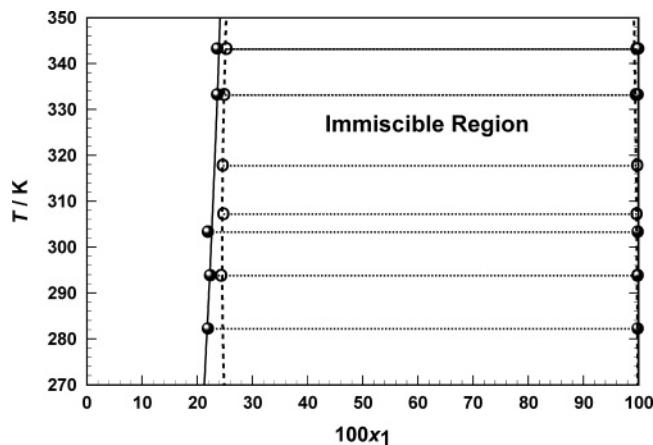


Figure 6. T_x phase diagram of the CFC-113 (CFC-113a) (1) + [emim][Tf₂N] (2) system: solid (CFC-113) and open (CFC-113a) circles, experimental LLE data; solid (CFC-113) and dotted (CFC-113a) lines, the present NRTL model calculations; solid (CFC-113) and broken (CFC-113a) horizontal lines, experimental LLE tie lines.

K and (279 ± 1) K at mole fractions of 97.0 % HCFC-123 and 96.1 % HCFC-123a, respectively. For the cases of HCFC-124 and HCFC-124a + [emim][Tf₂N], we have calculated LCSTs at about (281 ± 2) K and (269 ± 2) K at mole fractions of 94.0 % HCFC-124 and 92.0 % HCFC-124a, respectively. For the cases of HFC-134 and HFC-134a + [emim][Tf₂N], we have calculated LCSTs at about (356 ± 1) K and (328 ± 2) K at mole fractions of 96.5 % HFC-134 and 92.0 % HFC-134a, respectively. The halocarbon (HCFC-123, HCFC-124, and HFC-134) isomers + [emim][Tf₂N] systems belong to the Type-V fluid behavior, according to the classification of Scott and van Konynenburg,³⁴ and this is similar to the case of other HFC^{17–19} and CO₂^{22,35,36} containing systems that we have studied in RTILs.

Interesting phenomena observed with the CFC-113 and CFC-113a + [emim][Tf₂N] binary systems were density inversions between a temperature of about (318 and 333) K. As shown in Table 6 at $T \leq 318$ K, the lower liquid phase (L') contains essentially pure CFC-113 or CFC-113a; however, at $T \geq 333$ K, the upper liquid phase (L) contains essentially pure CFC-113 or CFC-113a. The liquid densities for CFC-113, CFC-113a, and [emim][Tf₂N] at 325 K are almost identical (1.498, 1.497, and 1.492 g·cm⁻³, respectively^{27–29}). Knowing the mole fraction of CFC-113 isomers in each phase, we can calculate that the upper and lower liquid phases have almost the same density at 325 K. When the temperature decreases ($T \leq 318$ K), the CFC-113 isomer-rich phase is heavier and sinks to the bottom, and when the temperature increases ($T \geq 333$ K), the CFC-113 isomer-rich phase is lighter and floats to the top. This is an interesting example of how the lack of a density difference between the two liquid phases can simulate a zero-gravity situation on Earth for studying mixing without requiring the environment of space. In this case, the surface tension effects dominate which led to measurement difficulties when trying to separate the two liquid phases. Typically, the time required for the heavier phase to completely settle to the bottom took a few hours, but in this case a few days were required along with slightly tilting and shaking the sample containers to help overcome surface tension effects which prevented the two liquids from forming distinct, measurable phases. A similar density inversion was observed in our previous work using HCFC-123 isomers mixed with [bmim][PF₆].²¹ In addition, a significant increase in the solubility of CFC-113 and HCFC-

123 was observed with mixtures prepared using [emim][Tf₂N] compared with our initial work using [bmim][PF₆],²¹ and this fact provides further evidence that ionic liquid structures (particularly anions) can be optimized to improve separation processes for halogenated compounds such as HFCs.^{12–15}

A few other interesting observations that are not widely known about these fascinating compounds (halocarbon isomers) are the freezing points. For example, those for CFC-113 and CFC-113a are quite different, (238.15 and 287.35) K, respectively, although the normal boiling points are almost identical, (320.74 and 319.31) K, respectively. This became immediately apparent when measuring the LLE behavior as the CFC-113a samples were solidified at 282 K while the CFC-113 samples remained liquid; therefore, this explains the lack of LLE data at 282 K in Table 6 for the CFC-113a isomer + [emim][Tf₂N]. Also, it should be noted that three isomers exist for HCFC-123 (CHCl₂–CF₃, HCFC-123; CHClF–CClF₂, HCFC-123a; and CHF₂–CFCl₂, HCFC-123b). HCFC-123b was, however, not obtainable from any source and not easily synthesized, so it was not included in this study, although it would be interesting to know how this compound interacts with ionic liquids such as [emim][Tf₂N], particularly because the normal boiling point is somewhat different from the other isomers (HCFC-123, $T_b = 300.97$ K; HCFC-123a, $T_b = 301.35$ K; and HCFC-123b, $T_b = 303.35$ K).^{37–44}

The present VLE data (CFC-114, HCFC-124, and HFC-134 isomers) have been well correlated using our EOS model^{19,22} (see Supporting Information for details) which was used to make predictions of LLE behavior. The measured LLE data for the low-pressure halocarbons (CFC-113 and HCFC-123 isomers) have been well correlated using the nonelectrolyte NRTL solution model^{13,23,24} (see Supporting Information for details). In this respect, needless to say, it is important to always check the experimental data with a proper *thermodynamic* model (not just an empirical fitting function), to validate the consistency of experiments. However, it must be mentioned that the LLE correlation for CFC-113 and HCFC-123 isomers should not be used beyond the experimentally measured temperature range. Solution activity models such as NRTL are good for data correlation as shown in Figures 5 and 6 but are not reliable for prediction beyond the experimental measurements as discussed in our previous paper.²⁴

More reliable predictions of large-scale (global) phase behaviors may be made using proper equations of state, which have been described in ref 19. Negative excess molar volumes in [emim][Tf₂N]-rich side solutions have been observed for all the present systems and in some cases are largely negative (e.g., HFC-134a + [emim][Tf₂N] from $(-9$ to $-15)$ cm³·mol⁻¹). These values are similar to our previous studies of other binary systems containing HFCs^{17–19} and CO₂^{22,35,36} + ionic liquids. This clearly indicates that RTILs (e.g., [emim][Tf₂N] and [bmim][PF₆]) with gases such as HFCs and CO₂ have quite large negative excess molar volumes compared with what have been reported with ordinary liquid mixtures (typically about $(0$ to $\pm 3)$ cm³·mol⁻¹).⁴⁵ This poses a unique and interesting challenge for theoretical modelers to explain this phenomenon. One possible explanation by Huang et al.⁴⁶ for the CO₂ + [bmim][PF₆] system indicates that small angular rearrangements of the anion are occurring which create localized cavities that allow CO₂ to fit above and below the imidazolium ring without much change from the molar volume of pure [bmim][PF₆]. Similar rearrangements may be occurring with HFCs in RTILs such as [emim][Tf₂N], and an additional force such as hydrogen bonding may also be involved.

Conclusions

Solubility behaviors of five isomer pairs (CFC-113 and CFC-113a; CFC-114 and CFC-114a; HCFC-123 and HCFC-123a; HCFC-124 and HCFC-124a; HFC-134 and HFC-134a) in RTIL ([emim][Tf₂N]) have been studied over a temperature range of about (283 to 348) K using the gravimetric microbalance, volumetric, and cloud-point methods. All cases exhibit liquid–liquid-phase separations. For the case of the HFC-134 isomers, the difference in solubility of the two isomers in the RTIL is large enough that separation using [emim][Tf₂N] as an entrainer in an extractive distillation application is practical. The minor differences for the other isomer pairs (CFC-113, CFC-114, HCFC-123, and HCFC-124) make separation using [emim]-[Tf₂N] impractical.

The hydrogen substitution (Cl → H) significantly increased the solubility in [emim][Tf₂N]: for CFCs to HCFCs, CFC-113 (CFCl₂–CF₂Cl) → HCFC-123a (CHClF–CF₂Cl), CFC-113a (CCl₃–CF₃) → HCFC-123 (CHCl₂–CF₃), CFC-114 (CF₂Cl–CF₂Cl) → HCFC-124a (CHF₂–CF₂Cl), CFC-114a (CFCl₂–CF₃) → HCFC-124 (CHFCl–CF₃), and for HCFCs to HFCs, HCFC-124a (CHF₂–CF₂Cl) → HFC-134 (CHF₂–CHF₂), HCFC-124 (CHFCl–CF₃) → HFC-134a (CH₂F–CF₃).

The halocarbon (HCFC-123, HCFC-124, and HFC-134) isomers + [emim][Tf₂N] binary systems exhibit LCSTs and belong to the Type-V fluid behavior. Experimental VLE and LLE data were well correlated with EOS and NRTL activity solution models; however, in the case of the NRTL model, the correlation is only valid for the measured temperature range. Negative excess molar volumes in [emim][Tf₂N]-rich side solutions have been observed for all the present systems and in some cases are largely negative (e.g., HFC-134a + [emim]-[Tf₂N] from (–9 to –15) cm³·mol^{–1}) which are similar to our previous studies with other HFCs and CO₂ in ionic liquids.

Acknowledgment

The authors thank Mr. Brian L. Wells and Mr. Joe Nestlerode at the DuPont Experimental Station for their assistance with the gas solubility measurements and LLE measurements, respectively. They appreciate Dr. Allen C. Sievert (DuPont Fluorochemicals) who kindly provided the CFC-113, CFC-113a, and HCFC-123 samples and Dr. Lam H. Leung (DuPont Corporate Center Analytical Science) for the GCMS analysis. They also thank Dr. Marcia L. Huber (National Institute of Standards and Technology, Boulder, Colorado) for kindly providing several references for HCFC-123a and other halocarbon physical properties (refs 37 to 44).

Supporting Information Available:

Information on thermodynamic models 1 and 2 and Tables S1 to S3. This information is available free of charge via the Internet at <http://pubs.acs.org>.

Literature Cited

- Seiler, M.; Jork, C.; Kavarnou, A.; Arlt, W.; Hirsch, R. Separation of Azeotropic Mixtures Using Hyperbranched Polymers or Ionic Liquids. *AIChE J.* **2004**, *50* (10), 2439–2454.
- Scovazzo, P.; Kieft, J.; Finan, D. A.; Koval, C.; DuBois, D.; Noble, R. Gas separations using non-hexafluorophosphate [PF₆[–]] anion supported ionic liquid membranes. *J. Membr. Sci.* **2004**, *238*, 57–63.
- Zhang, S.; Zhang, Q.; Zhang, Z. C. Extractive Desulfurization and Denitrogenation of Fuels Using Ionic Liquids. *Ind. Eng. Chem. Res.* **2004**, *43*, 614–622.
- Lei, Z.; Arlt, W.; Wasserscheid, P. Separation of 1-hexene and n-hexane with ionic liquids. *Fluid Phase Equilib.* **2006**, *241*, 290–299.
- Marták J.; Schlosser, S. Extraction of lactic acid by phosphonium ionic liquids. *Sep. Purif. Technol.* **2006**, doi:10.1016/j.seppur.2006.09.013.
- Anjan, S. Ionic Liquids for Aromatic Extraction: Are They Ready? *Chem. Eng. Progress* **2006**, *12*, 30–39.
- Wasserscheid, P.; Welton, T., Eds. *Ionic Liquids in Synthesis*; Wiley-VCH: Weinheim, 2003.
- Rogers, R. D.; Seddon, K. R.; Volkov, S., Eds. *Green Industrial Applications of Ionic Liquids*; NATO Science Series; Kluwer Academic Publishers: Boston, 2002; Vol. 92.
- Rogers, R. D.; Seddon, K. R., Eds. *Ionic Liquids IIIA: Fundamentals, Progress, Challenges, and Opportunities - Properties and Structure*; ACS Symposium Series 901, Oxford University Press: Washington, DC, 2005.
- Rogers, R. D.; Seddon, K. R., Eds. *Ionic Liquids IIIB: Fundamentals, Progress, Challenges, and Opportunities – Transformations and Processes*; ACS Symposium Series 902, Oxford University Press: Washington, DC, 2005.
- Yokozeki, A.; Shiflett, M. B.; Hydrogen Purification Using Room-Temperature Ionic Liquids. *Appl. Energy* **2007**, *84* (3), 351–361.
- Shiflett, M. B.; Yokozeki, A. Separation of difluoromethane and pentafluoroethane by extractive distillation using ionic liquid. *Chem. Today* **2006**, *24* (2), 28–30.
- Shiflett, M. B.; Yokozeki, A. Solubility and Diffusivity of Hydrofluorocarbons in Room-Temperature Ionic Liquids. *AIChE J.* **2006**, *52* (3), 1205–1219.
- Shiflett, M. B.; Junk, C. P.; Harmer, M. A.; Yokozeki, A. Solubility and Diffusivity of Difluoromethane in Room-Temperature Ionic Liquids. *J. Chem. Eng. Data* **2006**, *51* (2), 483–495.
- Shiflett, M. B.; Junk, C. P.; Harmer, M. A.; Yokozeki, A. Solubility and Diffusivity of 1,1,1,2-tetrafluoroethane in Room-Temperature Ionic Liquids. *Fluid Phase Equilib.* **2006**, *242*, 220–232.
- Shiflett, M. B.; Yokozeki, A. Gaseous Absorption of Fluoromethane, Fluoroethane, and 1,1,2,2-Tetrafluoroethane in 1-butyl-3-methylimidazolium Hexafluorophosphate. *Ind. Chem. Eng. Res.* **2006**, *45* (18), 6375–6382.
- Shiflett, M. B.; Yokozeki, A. Vapor–Liquid–Liquid Equilibria of Pentafluoroethane and Ionic Liquid [bmim][PF₆] Mixtures studied with the Volumetric Method. *J. Phys. Chem. B* **2006**, *110* (29), 14436–14443.
- Shiflett, M. B.; Yokozeki, A. Vapor–Liquid–Liquid Equilibria of Hydrofluorocarbons and 1-Butyl-3-methylimidazolium Hexafluorophosphate. *J. Chem. Eng. Data* **2006**, *51* (5), 1931–1939.
- Yokozeki, A.; Shiflett, M. B. Global Phase Behaviors of Trifluoromethane in Room-Temperature Ionic Liquid [bmim][PF₆]. *AIChE J.* **2006**, *52* (11), 3952–3957.
- Shiflett, M. B.; Yokozeki, A. Phase Equilibria of Hydrofluorocarbon-4310mee Mixtures with Ionic Liquids: Miscibility of Threo- and Erythro- Diastereomers in Ionic Liquids. *Ind. Eng. Chem. Res.* **2007**, submitted.
- Shiflett, M. B.; Yokozeki, A. Hydrogen Substitution Effect on the Solubility of Perhalogenated Compounds in Ionic Liquid [bmim][PF₆]. *Fluid Phase Equilib.* **2007**, in press.
- Shiflett, M. B.; Yokozeki, A. Solubilities and Diffusivities of Carbon Dioxide in Ionic Liquids: [bmim][PF₆] and [bmim][BF₄]. *Ind. Eng. Chem. Res.* **2005**, *44*, 4453–4464.
- Poling, B. E.; Prausnitz, J. M.; O’Connell, J. P. *The Properties of Gases and Liquids*, 5th ed.; McGraw-Hill: New York, 2001.
- Shiflett, M. B.; Yokozeki, A. Liquid–Liquid Equilibria in Binary Mixtures of 1,3-Propanediol + Ionic Liquids [bmim][PF₆], [bmim][BF₄], and [emim][BF₄]. *J. Chem. Eng. Data* **2007**, *52*, 1302–1306.
- Covalent Associates, Inc., Woburn, MA. www.covalentassociates.com.
- Schwarzkopf Microanalytical Laboratory, Woodside, NY. www.schwarzkopfmicrolab.com.
- Krummen, M.; Wasserscheid, P.; Gmehling, J. Measurement of Activity Coefficients at Infinite Dilution in Ionic Liquids Using the Dilutor Technique. *J. Chem. Eng. Data* **2002**, *47*, 1411.
- Lemmon, E. W.; McLinden, M. O.; Huber, M. L. *NIST reference fluid thermodynamic and transport properties - REFPROP*, version 7.0, users’ guide; U. S. Department of Commerce, Technology Administration, National Institute of Standards and Technology, Standard Reference Data Program: Gaithersburg, MD, 2002.
- Yokozeki, A. *BLENDY computer program*, version 3; DuPont Fluoroproducts: Wilmington, DE, 1992.
- Reid, R. C.; Prausnitz, J. M.; Poling, B. E. *The Properties of Gases and Liquids*, 4th ed.; McGraw-Hill: New York, 1987.
- Chae, H. B.; Schmidt, J. W.; Moldover, M. R. Alternative Refrigerants R123a, R134, R141b, R142b, and R152a: Critical Temperature, Refractive Index, Surface Tension, and Estimates of Liquid, Vapor, and Critical Densities. *J. Phys. Chem.* **1990**, *94*, 8840–8845.
- Henne, A. L.; Ladd, E. C. Fluorochloroethanes and Fluorochloroethylenes. II. *J. Am. Chem. Soc.* **1936**, *58*, 42–403.
- Park, J. D.; Lycan, W. R.; Lacher, J. R. The Addition Products of Trifluoroethylene. *J. Am. Chem. Soc.* **1951**, *73*, 711–712.

- (34) van Knoyenberg, P. H.; Scott, R. L. Critical Lines and Phase Equilibria In Binary Van Der Waals Mixtures. *Philos. Trans.* **1980**, A298, 495–540.
- (35) Shiflett, M. B.; Yokozeki, A. Solubility of CO₂ in Room-Temperature Ionic Liquid [hmim][Tf₂N]. *J. Phys. Chem. B* **2007**, 111 (8), 2070–2074.
- (36) Shiflett, M. B.; Kasprzak, D. J.; Junk, C. P.; Yokozeki, A. Phase Behavior of Carbon Dioxide + [bmim][Ac] Mixtures. *J. Chem. Thermodyn.* **2007**, doi:10.1016/j.jct.2007.06.003.
- (37) Kubota, H.; Yamashita, T.; Tanaka, Y.; Makita, T. Vapor pressures of new fluorocarbons. *Int. J. Thermophys.* **1989**, 10 (3), 629–637.
- (38) Yokoyama, C.; Takahashi, S. Saturated liquid densities of 2,2-dichloro-1,1,1-trifluoroethane (HCFC-123), 1,2-dichloro-1,2,2-trifluoroethane (HCFC-123a), 1,1,1,2-tetrafluoroethane (HFC-134a), and 1,1,1-trifluoroethane (HFC-143a). *Fluid Phase Equilib.* **1991**, 67, 227–240.
- (39) Takagi, T.; Kusunoki, M.; Hongo, M. Speed of Sound in liquid 1,2-dichloro-1,2,2-trifluoroethane from 283 to 373 K and up to 75 MPa. *J. Chem. Eng. Data* **1992**, 37, 39–41.
- (40) Kumagai, A.; Yokoyama, C. Revised viscosities of saturated liquid halocarbon refrigerants from 273 to 353 K. *Int. J. Thermophys.* **2000**, 21 (4), 909–912.
- (41) Defibaugh, D. R.; Moldover, M. R. Compressed and saturated liquid densities for 18 halogenated organic compounds. *J. Chem. Eng. Data* **1997**, 42 (1), 160–168.
- (42) Malhotra, R.; Woolf, L. A. PVT property measurements for liquid 1,2-dichloro-1,2,2-trifluoroethane from 278 to 338 K. *J. Chem. Eng. Data* **1996**, 41 (2), 254–257.
- (43) Meyer, C. W.; Morrison, G. Dipole-Moments of 7 Refrigerants. *J. Chem. Eng. Data* **1991**, 36 (4), 409–413.
- (44) Goodwin, A. R. H.; Moldover, M. R. Thermophysical properties of gaseous refrigerants from speed-of-sound measurements. 3. Results for 1,1-dichloro-2,2,2-trifluoroethane (CHCl₂-CF₃) and 1,2-dichloro-1,2,2-trifluoroethane (CHClF-CClF₂). *J. Chem. Phys.* **1991**, 95 (7), 5236–5242.
- (45) Rowlinson, J. S.; Swinton, F. L. *Liquids and Liquid Mixtures*, 3rd ed.; Butterworth: London, 1982.
- (46) Huang, X.; Margulis, C.; Li, Y.; Berne, B. J. Why is the Partial Molar Volume of CO₂ So Small When Dissolved in a Room Temperature Ionic Liquid? Structure and Dynamics of CO₂ Dissolved in [Bmim⁺][PF₆⁻]. *J. Am. Chem. Soc.* **2005**, 127, 17842–17851.

Received for review May 26, 2007. Accepted July 9, 2007. The present work was supported by DuPont Central Research and Development.

JE700295E